JOURNAL OF GUIDANCE, CONTROL, AND DYNAMICS
Vol. 26, No. 2, March–April 2003

Low-Order Equivalent System Identification for the Tu-144LL Supersonic Transport Aircraft

Eugene A. Morelli*
NASA Langley Research Center, Hampton, Virginia 23681-2199

Low-order equivalent system models were identified from flight-test data for the Tu-144LL supersonic transport aircraft. Flight-test maneuvers were executed by Russian and American test pilots flying the aircraft from Zhukovsky airfield outside Moscow, Russia. Flight tests included longitudinal and lateral/directional maneuvers at supersonic cruise flight conditions. Piloted frequency sweeps and multistep maneuvers were used to generate data for closed-loop low-order equivalent system modeling. Parameters in these models were estimated using a high-accuracy Fourier transform with selectable frequency capability and an equation-error/output-error (EE/OE) formulation in the frequency domain. Results were compared to parameter estimates obtained using spectral estimation and subsequent least-squares fit to frequency response data used for Bode plots, as implemented in the commercial software package CIFER®. Modeling results from the two methods agreed well for both a frequency sweep and multiple concatenated multistep maneuvers. For a single multistep maneuver, only the EE/OE method gave an adequate model fit with good prediction capability. Closed-loop low-order equivalent system identification results for the Tu-144LL at several different flight conditions were computed and tabulated.

Nomenclature

e	=	equation error
h	=	altitude, ft
I_x, I_y, I_z	=	body-axis moments of inertia, slug · ft^2
J	=	cost function
j	=	imaginary number $\sqrt{(-1)}$
M	=	Mach number
m	=	number of discrete frequencies
p, q, r	=	roll, pitch, and yaw rates, deg/s
s	=	Laplace transform variable
T_R	=	roll mode time constant, s
u	=	input
v	=	output error
w	=	weight, lbf
$x_{\text{c.g.}}$	=	longitudinal center of gravity position
y	=	model output
z	=	measured output
α	=	angle of attack, deg
ζ	=	damping ratio
η	=	pilot control deflection, cm
τ	=	equivalent time delay, s
ω	=	frequency, rad/s
$\angle$	=	phase angle, deg
$\lvert\ \rvert$	=	magnitude of a complex number

Subscripts

a	=	lateral stick
DR	=	Dutch roll
e	=	longitudinal stick
EE	=	equation error
LOES	=	low-order equivalent system
LS	=	least squares
OE	=	output error
o	=	nominal or trim value
r	=	rudder pedal
SP	=	short period

Superscripts

†	=	complex conjugate transpose
$\sim$	=	Laplace or Fourier transform

Received 28 August 2000; revision received 5 November 2002; accepted for publication 6 November 2002.

*Research Engineer, Dynamics and Control Branch, MS 132. Senior Member AIAA.

Introduction

As part of the NASA High-Speed Research (HSR) program, the Tupolev Aircraft Company in Russia was commissioned to refurbish, reengine, and instrument an out-of-service Tu-144D supersonic transport aircraft for use as a supersonic flying laboratory. The modified aircraft, designated the Tu-144LL, was operated from Zhukovsky airfield, near Moscow, Russia.

Flight-test data were collected for six experimental investigations related to high-speed research. One of the experimental investigations involved closed-loop flying qualities. Flight testing began with 19 phase 1 flights in 1996–1997, flown exclusively by Tupolev Aircraft Company pilots.

Reference 1 contains results of longitudinal, lateral, and directional closed-loop low-order equivalent system (LOES) modeling based on the phase 1 flight-test data, using an equation-error method in the frequency domain.[1–3] The LOES model characterizes the linearized closed-loop dynamic response of the airframe and control system as it appears to the pilot. The form of the LOES model is the same as that for an open-loop unaugmented airplane with classical dynamic modes, except that the inputs are pilot controls with equivalent time delays, instead of control surface deflections. Equivalent time delay is introduced to account for time delay resulting from control system discretization, high-frequency control system dynamics, and various nonlinearities, such as control surface rate limiting. LOES models for the aircraft closed-loop dynamic response are fit over the frequency band corresponding to typical pilot inputs, 0.1–10 rad/s.

Many flight-test research programs[4–7] have studied the correlation between LOES model parameters and pilot opinion for augmented aircraft dynamic responses that are, in reality, high order and/or nonlinear. This correlation provides guidance to control system designers regarding the closed-loop linear dynamics preferred by pilots. LOES models identified from flight-test data can be used for validating control law designs and verifying specification compliance because the LOES model represents the achieved linearized closed-loop dynamics of the aircraft. In addition, LOES models can be used for rudimentary simulation within the limited flight envelope where the models are valid.

A second phase of flight testing for closed-loop flying qualities research was conducted on the Tu-144LL in the fall of 1998. Phase 2 testing included four flights, one subsonic flight with an all-Russian

crew (flight 20), one subsonic flight with an American evaluation pilot (flight 21), and two supersonic flights with American evaluation pilots (flights 22 and 23). These flights included flying qualities evaluation tasks, approaches, and special maneuvers designed to collect data for closed-loop LOES modeling. Reference 8 contains extensive information on the Tu-144LL aircraft, flight profiles, and maneuvers for these flights, including qualitative pilot commentary and narrative flight summaries from the American evaluation pilots.

The work described here examined LOES modeling based on the Tu-144LL phase 2 flight-test data using an equation-error/output-error technique in the frequency domain and a high-accuracy Fourier transform with selectable frequency range and resolution.[2,9] Results were compared with LOES models obtained from a least-squares fit to a nonparametric estimate of the Bode plot, using commercially available software called CIFER® (Refs. 10–12). Correlation of the analytical LOES modeling results with pilot opinion was not done because the pilots gave only qualitative narrative assessments.

The next section describes the two LOES model parameter estimation techniques used. Next, LOES modeling issues are examined by applying the two parameter estimation techniques to Tu-144LL phase 2 flight-test data. Finally, LOES modeling results for the Tu-144LL phase 2 flights are computed and tabulated.

Methods

The structure of the LOES model is fixed a priori to correspond to classical linearized aircraft dynamics with an input time delay. For the short period longitudinal dynamic mode, the closed-loop pitch rate response to longitudinal stick deflection is modeled in transfer function form as[4]

$$\tilde{q} = \frac{K_{\tilde{\theta}}(s + 1/T_{\theta_2})e^{-\tau_e s}}{\left(s^2 + 2\zeta_{\mathrm{SP}}\omega_{\mathrm{SP}}s + \omega_{\mathrm{SP}}^2\right)}\tilde{\eta}_e \tag{1}$$

For lateral/directional closed-loop dynamics, the LOES models for roll rate and yaw rate responses are

$$\tilde{p} = \frac{K_{p_1}\left(s^2 + 2\omega_{p_1}\zeta_{p_1}s + \omega_{p_1}^2\right)e^{-\tau_r s}}{(s + 1/T_R)\left(s^2 + 2\zeta_{\mathrm{DR}}\omega_{\mathrm{DR}}s + \omega_{\mathrm{DR}}^2\right)}\tilde{\eta}_r + \frac{K_{p_2}\left(s^2 + 2\omega_{p_2}\zeta_{p_2}s + \omega_{p_2}^2\right)e^{-\tau_a s}}{(s + 1/T_R)\left(s^2 + 2\zeta_{\mathrm{DR}}\omega_{\mathrm{DR}}s + \omega_{\mathrm{DR}}^2\right)}\tilde{\eta}_a \tag{2}$$

$$\tilde{r} = \frac{K_{r_1}\left(s^2 + 2\omega_{r_1}\zeta_{r_1}s + \omega_{r_1}^2\right)e^{-\tau_r s}}{(s + 1/T_R)\left(s^2 + 2\zeta_{\mathrm{DR}}\omega_{\mathrm{DR}}s + \omega_{\mathrm{DR}}^2\right)}\tilde{\eta}_r + \frac{K_{r_2}\left(s^2 + 2\omega_{r_2}\zeta_{r_2}s + \omega_{r_2}^2\right)e^{-\tau_a s}}{(s + 1/T_R)\left(s^2 + 2\zeta_{\mathrm{DR}}\omega_{\mathrm{DR}}s + \omega_{\mathrm{DR}}^2\right)}\tilde{\eta}_a \tag{3}$$

Apart from the equivalent time delays on the inputs, the forms of the models in Eqs. (2) and (3) follow from classical linearized aircraft lateral/directional dynamics model, omitting the gravity term in the side-force equation.

The problem addressed in this work is the accurate estimation of the model parameters in Eqs. (1–3) using measured input–output flight-test data. The idea is to match the measured outputs or output time derivatives with corresponding quantities from the model by adjusting model parameters to minimize a measure of fit error. The measure of fit error is the sum of the squared deviations between model quantity and measured quantity, or an analogous weighted sum of such fit error measures. Several methods exist for estimating model parameters based on measured data, both in the time domain[13,14] and the frequency domain.[1–4,10–12]

For identification purposes, Eqs. (1–3) can be reparameterized as

$$\tilde{q} = \frac{(b_1 s + b_0)e^{-\tau_e s}}{\left(s^2 + a_1 s + a_0\right)}\tilde{\eta}_e \tag{4}$$

$$\tilde{p} = \frac{\left(d_2 s^2 + d_1 s + d_0\right)e^{-\tau_a s}}{\left(s^3 + c_2 s^2 + c_1 s + c_0\right)}\tilde{\eta}_a + \frac{\left(e_2 s^2 + e_1 s + e_0\right)e^{-\tau_r s}}{\left(s^3 + c_2 s^2 + c_1 s + c_0\right)}\tilde{\eta}_r \tag{5}$$

$$\tilde{r} = \frac{\left(f_2 s^2 + f_1 s + f_0\right)e^{-\tau_r s}}{\left(s^3 + c_2 s^2 + c_1 s + c_0\right)}\tilde{\eta}_r + \frac{\left(g_2 s^2 + g_1 s + g_0\right)e^{-\tau_a s}}{\left(s^3 + c_2 s^2 + c_1 s + c_0\right)}\tilde{\eta}_a \tag{6}$$

The relationship among the parameters in Eqs. (1–3) and Eqs. (4–6) can be found by direct comparison. All LOES modeling was done in the frequency domain because the equivalent time delay parameters can be estimated more easily and accurately in the frequency domain[2,10] than in the time domain.

In the literature,[4] the general recommendation for LOES modeling is to augment the angular rate measurements with additional output measurements, such as angle of attack, sideslip angle, and/or translational accelerations. For the Tu-144LL aircraft, data compatibility analysis[15,16] indicated that the measured angle of attack, sideslip angle, and translational accelerations contained significant systematic instrumentation errors. More details are given in the "Aircraft" section. Recent work[2] has suggested that accurate LOES modeling can be done using only body-axis angular rate measurements for the measured outputs. For these reasons, all of the LOES modeling done in this work used only the aircraft angular rate data for the measured outputs. Equations (4–6) define the model structures used.

Two methods were used to estimate the parameters in Eqs. (4–6) based on flight-test data. The first method, described in Refs. 10–12, involves computing a nonparametric estimate of the frequency response in the form of a Bode plot. Then, the model parameters in Eqs. (4–6) are adjusted to minimize the least-squares cost function:

$$J_{\mathrm{LS}} = \sum_{i=1}^{m}\left(\left[20\log_{10}\left|\frac{\tilde{z}(\omega_i)}{\tilde{u}(\omega_i)}\right| - 20\log_{10}\left|\frac{\tilde{y}(\omega_i)}{\tilde{u}(\omega_i)}\right|_{\mathrm{LOES}}\right]^2 + 0.0175\left\{\angle\left[\frac{\tilde{z}(\omega_i)}{\tilde{u}(\omega_i)}\right] - \angle\left[\frac{\tilde{y}(\omega_i)}{\tilde{u}(\omega_i)}\right]_{\mathrm{LOES}}\right\}^2\right) \tag{7}$$

Typically, the number of frequencies m is 50, and the frequencies are chosen to be evenly spaced on a logarithmic scale over the interval [0.1, 10] rad/s. Commercially available FORTRAN software called CIFER[10–12] was used to estimate LOES model parameters with this method.

The second method, described in Ref. 2, is a two-step approach using equation-error (EE) and output-error (OE) formulations in the frequency domain for the parameter estimation. For the EE formulation, the cost function is

$$J_{\mathrm{EE}} = \frac{1}{2}\sum_{i=1}^{m}\left|D(j\omega_i)\tilde{z}_i - N(j\omega_i)\tilde{u}_i e^{-j\omega_i\tau}\right|^2 = \frac{1}{2}\sum_{i=1}^{m}|\tilde{e}_i|^2 = \frac{1}{2}(\tilde{e}^{\dagger}\tilde{e}) \tag{8}$$

where $N(j\omega_i)$ and $D(j\omega_i)$ are the numerator and denominator polynomials of the transfer function, with $s = j\omega_i$. Accurate Fourier transforms for m arbitrary frequencies were computed using the method from Ref. 9. Parameter estimation results from the EE method were used as starting values for the OE method, which minimized the cost function:

$$J_{\mathrm{OE}} = \frac{1}{2}\sum_{i=1}^{m}|\tilde{z}_i - \tilde{y}_i|^2 = \frac{1}{2}\sum_{i=1}^{m}|\tilde{v}_i|^2 = \frac{1}{2}(\tilde{v}^{\dagger}\tilde{v}) \tag{9}$$

Final parameter estimates were from the OE formulation because of known favorable asymptotic properties.[13,14]

EE is much more robust to starting values of the parameters because the model output depends linearly on all model parameters except the equivalent time delay τ. For EE parameter estimation, all parameters except τ were estimated using a standard least-squares regression solution for frequency domain data.[2] The τ parameter was estimated using a one-dimensional search in a relaxation approach.[2] For this work, the EE method always converged quickly and without difficulty, using zeros for the starting values of all parameters.

Parameter estimates from the EE method provide good starting values for the OE method. The OE method needs good starting values for the parameters because the model output depends nonlinearly on the transfer function parameters, in addition to the equivalent time delay τ. The EE/OE sequence, therefore, gives parameter estimation results with good asymptotic properties, without requiring good starting values for the parameters. Estimated parameter standard errors do not require correction because the analysis in the frequency domain automatically accounts for colored residuals.[2,13,14] Both the EE and OE methods are nonlinear estimation problems for LOES modeling because of the equivalent time delay parameter. Details on the optimization methods used to find both EE and OE parameter estimates can be found in Ref. 2.

Any of the methods just described can be used for general multi-input/multi-output models. For the results given here, Eqs. (4–6) were used to identify LOES models from flight-test data. For multiple-output cases, cost function terms for each output were weighted according to residual variance estimates (see Ref. 2 or Ref. 3).

Important differences between the CIFER and EE/OE methods can be appreciated by examination of the cost functions in Eqs. (7–9). The CIFER method minimizes a cost comprised of the weighted sum of the squared difference between measured and model transfer function frequency response magnitude in decibels and phase angle in degrees. The first step in the CIFER method is nonparametric estimation of the transfer function frequency response in the form of a Bode plot, obtained using the ratio of estimates for the input–output cross-spectral density and input autospectral density. The two weighted terms in the cost involve nonlinear functions of the complex frequency response (magnitude in decibels and phase angle in degrees). Because the frequency response estimate is calculated from a ratio of spectral estimates, the accuracy of the estimated frequency response can degrade when the frequency content of the data is sparse. CIFER uses coherence weighting[10–12] in the parameter estimation to emphasize frequency domain data with good linearity and signal-to-noise ratio.

The EE/OE method uses high-accuracy, arbitrary frequency Fourier transforms directly and minimizes the square magnitude of the equation error or the output error with equal weighting of the real and imaginary parts of the complex quantities in the cost functions. Spectral content in the data influences parameter estimation results, according to the complex magnitude of the input–output data in the frequency domain. For the EE method, frequency scaling that depends only on the transfer function denominator order is applied to prevent overemphasizing high-frequency data.[2]

One other difference in the two methods that is not readily apparent from Eqs. (7–9) is that the frequencies were chosen to be evenly spaced on a logarithmic scale for the CIFER method, whereas the EE/OE method used evenly spaced values on an ordinary number line. Both methods used the frequency range [0.1, 10] rad/s. Although these choices of frequencies made the number of frequency points unequal for the two methods, this approach was taken because it represents how each method is normally applied in practice, which is of most interest to practitioners. The EE/OE method, therefore, used more data points at higher frequencies, whereas the CIFER method used more data points at lower frequencies. However, the CIFER method required repeated use of the time-domain data for the overlapping data windows of various lengths used to compute spectral estimates. The EE/OE method used the time-domain data only once, to compute the Fourier transform. Rather than try to balance the overall data usage of the two methods in some artificial way, the methods were simply applied as they would normally be used in practice.

For the shorter multistep flight-test maneuvers, the OE step of the EE/OE method used a priori information from the EE step in the OE parameter estimation, for the time delay parameter only. This involves including an extra term in the OE cost function, as follows:

$$J_{\mathrm{OE}} = \frac{1}{2}\sum_{i=1}^{m} |\tilde{z}_i - \tilde{y}_i|^2 + \frac{(\tau - \tau_{\mathrm{EE}})^2}{s^2_{\tau_{\mathrm{EE}}}} \qquad (10)$$

where τ_{EE} is the EE estimate of the equivalent time delay, and $s^2_{\tau_{\mathrm{EE}}}$ is the associated estimated parameter variance. This approach of including a priori information in the OE cost function has a Bayesian estimation interpretation, as discussed in Ref. 17. For the longitudinal short period LOES model, the equivalent time delay parameter has been found to have high correlations with all of the other LOES model parameters, unless there is sufficient data at both high and low frequencies relative to the natural frequency of the system.[2] Because the multistep data contain mainly data near the system natural frequency, a priori information for the equivalent time delay from the EE step must be included in the OE parameter estimation. For the frequency sweep maneuvers, the a priori information term for the equivalent time delay in the OE cost function was not required because these data contained a wide range of frequencies. The EE/OE software has the capability to incorporate a priori information for any or all of the model parameters in either the EE or the OE parameter estimation, in a manner analogous to that shown in Eq. (10) for the equivalent time delay parameter.

Reference 2 includes results demonstrating that relatively short multistep inputs can be used effectively for LOES modeling and includes application of the EE/OE method to some of the more troublesome LOES modeling cases from Refs. 4 and 6.

Details of the calculations and optimization methods used to find the parameter estimates that minimized the cost functions in Eqs. (7–9) can be found in Refs. 10–12 for the CIFER method and Ref. 2 for the EE/OE method.

Aircraft

The Tu-144LL test aircraft is a modified version of the Tupolev Aircraft Company Tu-144D cranked delta-wing supersonic transport. Modifications included installation of Kuznetsov NK-321 engines rated at 31,000 lbf static dry thrust and 55,000 lbf in afterburner at sea level and installation of flight-test instrumentation with a sampling rate of 32 Hz. A three-view of the Tu-144LL is shown in Fig. 1. Vehicle characteristics are summarized in Table 1. For cruise flight, the canards are retracted along the fuselage above and behind the cockpit, and the nose is raised. On approach, the canards are extended for slow flight, and the nose is drooped for enhanced visibility from the cockpit. The flight crew consisted of two pilots, a navigator, and a flight engineer. Details of the flight control system are available in Ref. 8.

Table 1 Tu-144LL vehicle characteristics

Parameter	Value
Length, ft	215.5
Height, wheels up, ft	42.2
Wingspan, ft	94.5
Wing area, ft^2	6769
Mean aerodynamic chord, ft	76.5
Maximum fuel, lbm	209,440
Estimated maximum range, nm	1620
Maximum Mach number	2.4

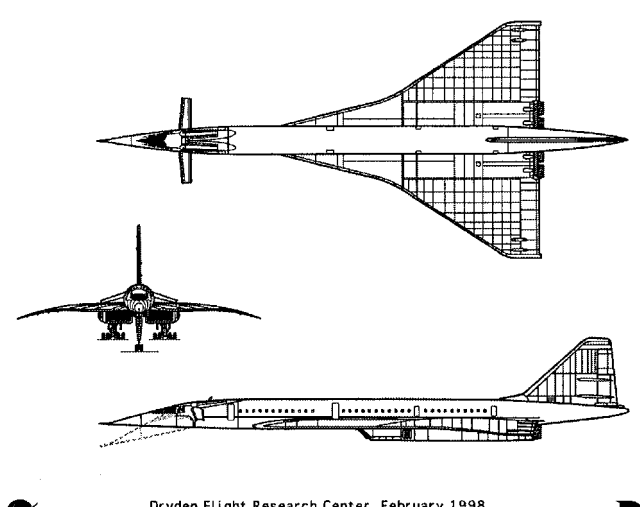

Fig. 1 Tu-144LL.

Air data on the Tu-144LL were obtained from production sensors, not specialized flight-test instrumentation, such as an air data probe. Data compatibility analysis[15,16] indicated that measurements of angle of attack and sideslip angle contained large systematic instrumentation errors relative to reconstructed values, including time skews and hysteresis effects. Because the translational acceleration measurements are the main influences on reconstructed values of angle of attack and sideslip angle, accuracy of the translational acceleration measurements was also in question. Angular rate data were found to be consistent with measured Euler angle data, from data compatibility analysis using the rotational kinematic equations only. Finally, there was some evidence to suggest that time skews were present in the measured input–output data, due to the instrumentation system. The main clue was an excessive time delay (~200 ms) between initial movement of control surfaces and angular rate response. However, it could not be determined conclusively what the instrumentation time skews were, or even if they were different from zero, and so the measured data for pilot inputs and angular rate outputs were analyzed as recorded.

Results

The first case studied was closed-loop identification of the Tu-144LL longitudinal short period LOES dynamics for supersonic cruise flight at Mach 1.93. The pilot applied a frequency sweep input to the longitudinal stick, shown in Fig. 2a. Measured pitch rate response is shown as the solid line in Fig. 2b. The dashed line on the same axes shows the computed pitch rate response to measured stick input, using the LOES model of Eq. (4) with parameters estimated using the EE/OE method. Figure 2c shows the output residual, which is the difference between the measured and computed pitch rate traces from Fig. 2b. Frequencies used in the data analysis were evenly spaced at 0.1 rad/s on the interval [0.1, 10] rad/s. The model fit in the frequency domain is shown in Figs. 2d and 2e. Figure 2 shows that the model fit in both the time and frequency domains was excellent. Estimated parameter values and standard errors for the identified $\tilde{q}/\tilde{\eta}_e$ LOES model are listed in the second column of Table 2. Estimated standard errors in Table 2 indicate that the model parameter accuracy was better than 8%, based on parameter estimate values, for all $\tilde{q}/\tilde{\eta}_e$ LOES model parameters.

CIFER was used with the same measured flight-test data to estimate model parameters in the same LOES model of Eq. (4). Results are given in the third column of Table 2. Comparison of the values in the second and third columns of Table 2 indicates that the results from CIFER agreed well with corresponding values from the EE/OE method. This gives confidence in the results because the two methods differ in formulation, data handling, cost function, and optimization technique, but still produced similar LOES modeling results. Because the CIFER model parameters were so close to the EE/OE model parameters, the computed pitch rate response from the CIFER model in both the time and frequency domains was nearly the same as the computed pitch rate response from the EE/OE model shown in Fig. 2. The Bode plot in Fig. 2d and 2e shows the excellent agreement of the LOES models identified using either EE/OE or CIFER to the measured data in the frequency domain.

Figure 3a shows a different kind of longitudinal stick input implemented by the pilot at approximately the same flight condition. This input was a modified doublet called a 2-1-1, which ideally consists of alternating pulses with pulse widths in the ratio 2-1-1.

Table 2 Tu-144LL longitudinal short period LOES modeling results, frequency sweep maneuver 23_1a, $\alpha_0 = 4.8$ deg, $M_0 = 1.93$, $x_{c.g.} = 0.46\bar{c}$, and $I_y = 1.44 \times 10^7$ slug · ft^2

Parameter	EE/OE estimate ±standard error	CIFER estimate ±standard error
b_1	0.353 ± 0.011	0.377 ± 0.022
b_2	0.106 ± 0.006	0.120 ± 0.014
a_1	0.932 ± 0.035	1.019 ± 0.121
a_0	1.970 ± 0.035	2.136 ± 0.139
τ_e	0.194 ± 0.014	0.190 ± 0.013
$1/T_{\theta_2}$	0.30	0.32
ζ_{SP}	0.33	0.35
ω_{SP}	1.40	1.46

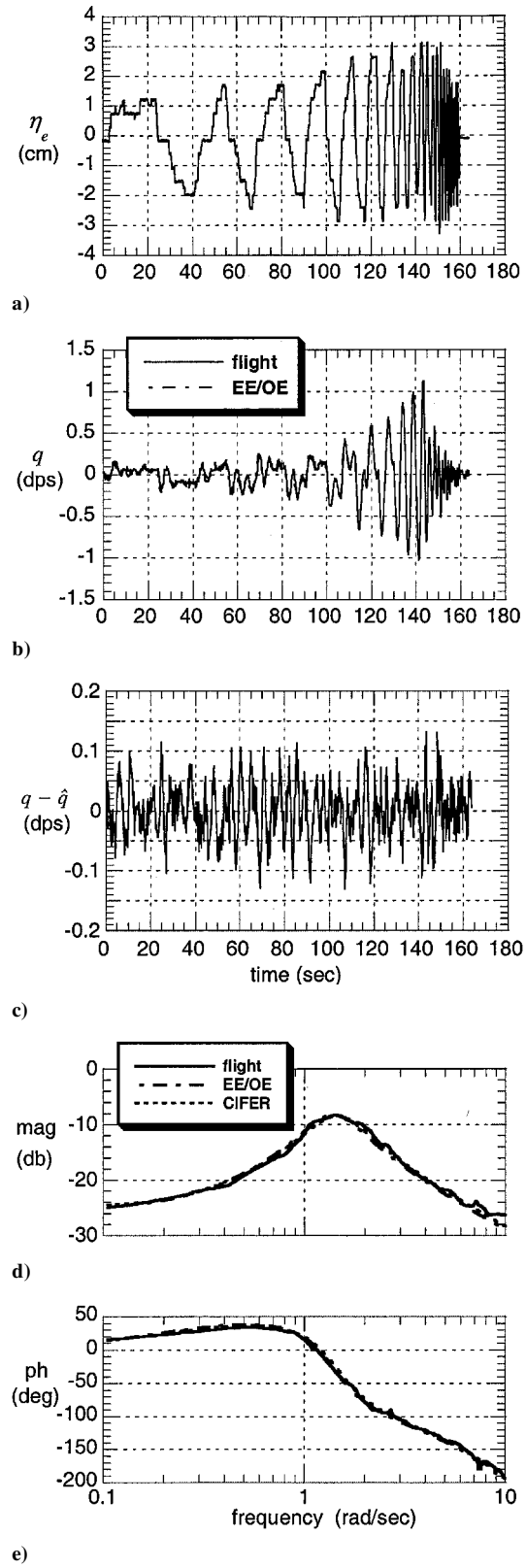

Fig. 2 Frequency sweep maneuver 23_1a, $\alpha_0 = 4.8$ deg, $M_0 = 1.93$, $x_{c.g.} = 0.46\bar{c}$, and $I_y = 1.44 \times 10^7$ slug · ft^2.

Inputs of this type are also called multistep inputs. The widths of the pulses were chosen so that the frequencies corresponding to the 2 and 1 pulses bracketed the a priori estimate of the natural frequency for the closed-loop short period mode. Data analysis results from phase 1 flights[1] at transonic cruise conditions were used to design the input pulse width and amplitude.

The EE/OE and CIFER methods were used to estimate LOES model parameters in Eq. (4), based on data from the 2-1-1 maneuver shown in Fig. 3. Table 3 contains the results. The EE/OE method

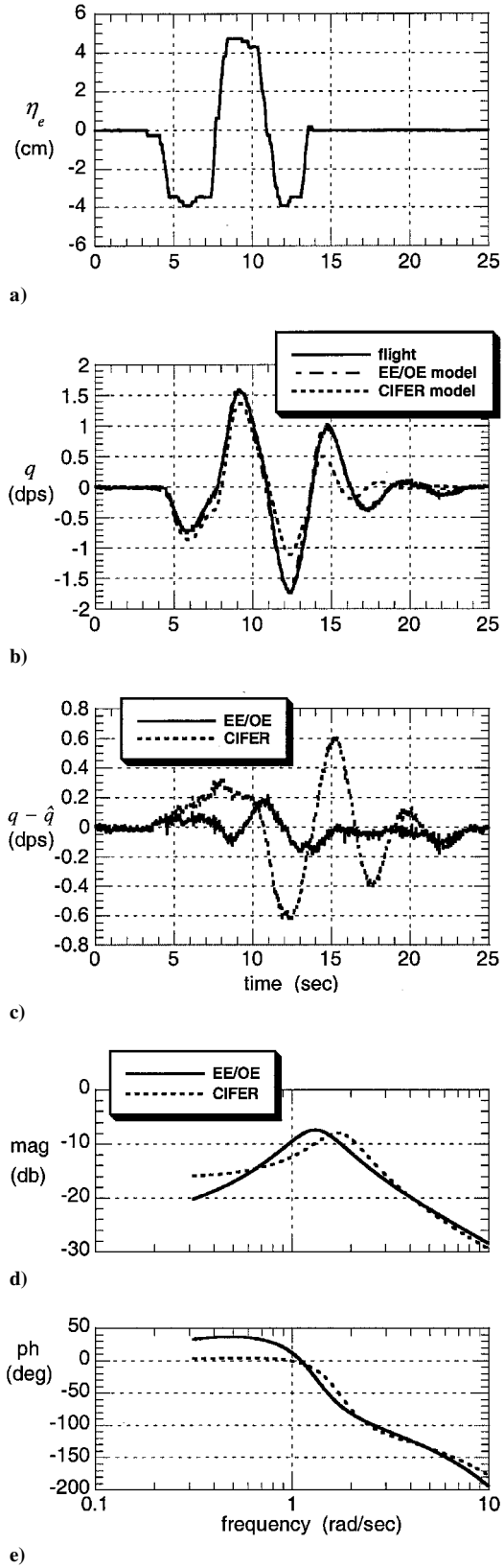

Fig. 3 Multistep 2-1-1 maneuver 22_4f, $\alpha_0 = 5.1$ deg, $M_0 = 1.90$, $x_{c.g.} = 0.046\bar{c}$, and $I_y = 1.41 \times 10^7$ slug · ft^2.

produced LOES model parameter estimates close to those estimated using the frequency sweep input at approximately the same flight condition (cf., the second column of Tables 2 and 3). The small discrepancies in the parameter estimates could be due to slight differences in flight conditions and mass properties that existed between the maneuvers in Figs. 2 and 3. Figures 3b and 3c show a good time-domain match to the measured pitch rate for the EE/OE model. CIFER parameter estimates in the third column of Table 3 were different than the EE/OE values, mainly because the 2-1-1 data did not provide sufficient power across the LOES modeling frequency range for an accurate Bode plot estimate based on spectral estimates. Figure 3 shows the corresponding time-domain comparison to the pitch rate measurement for the CIFER model identified using data from the 2-1-1 maneuver in Fig. 3, which is maneuver 22_4f. Figure 3c shows the time-domain residuals for both the CIFER model and the EE/OE model, indicating that the EE/OE model achieved a better match to the measured pitch rate data. The Bode plots in Figs. 3d and 3e show that the EE/OE method identified a different dynamic system than CIFER, based on the same data.

Table 3 Tu-144LL longitudinal short period LOES modeling results, 2-1-1 maneuvers, $\alpha_0 = 5.1$ deg, $M_0 = 1.90$, $x_{c.g.} = 0.46\bar{c}$, and $I_y = 1.41 \times 10^7$ slug · ft^2

Parameter	EE/OE[a] estimate ±standard error	CIFER[a] estimate ±standard error	CIFER[b] estimate ±standard error
b_1	0.375 ± 0.014	0.325 ± 0.025	0.434 ± 0.025
b_0	0.114 ± 0.008	0.484 ± 0.075	0.150 ± 0.032
a_1	0.905 ± 0.032	1.072 ± 0.118	1.088 ± 0.116
a_0	1.746 ± 0.031	3.173 ± 0.288	1.708 ± 0.142
τ_e	0.188 ± 0.024	0.149 ± 0.016	0.182 ± 0.014
$1/T_{\theta_2}$	0.30	1.49	0.35
ζ_{SP}	0.34	0.30	0.42
ω_{SP}	1.32	1.78	1.31

[a]Maneuver 22_4f. [b]Maneuvers 22_4a,b,f.

The CIFER method was not designed to work with data of this type. Results from CIFER improved and approached the EE/OE results when additional 2-1-1 maneuvers at the same flight condition were concatenated for the analysis, allowing additional averaging from the data windows, which improved the accuracy of the spectral estimation. Additional 2-1-1 maneuvers 22_4a and 22_4b were concatenated to the original single maneuver 22_4f for another CIFER analysis. The results shown in the fourth column of Table 3 are in good agreement with the EE/OE results, and Fig. 4 shows a good match to the pitch rate measurement. The multiple-maneuver CIFER results are denoted by CIFER 4abf, and the EE/OE results using data from maneuver 22_4f only are denoted EE/OE 4f. The EE/OE results plotted in Figs. 3 and 4 are the same. The Bode plot in Figs. 4c and 4d indicates that the CIFER model identified from the concatenated maneuvers 22_4a, 22_4b, and 22_4f was close to the model identified using the EE/OE method based on data from a single 2-1-1 maneuver 22_4f. The CIFER model, therefore, works well for 2-1-1 maneuvers also, given sufficient data for good spectral estimates. The EE/OE method is less sensitive to the data volume because Fourier transforms are used directly, instead of spectral estimates. This allows the EE/OE method to identify LOES models accurately using data from either a frequency sweep or a much shorter single 2-1-1 maneuver.

The EE/OE method can also be used with multiple maneuvers. For this case, results from the EE/OE method using concatenated data from maneuvers 22_4a, 22_4b, and 22_4f were similar to those given in the second column of Table 3, which were based on data from maneuver 22_4f alone.

Flight time required for the 2-1-1 maneuver in Fig. 3 is approximately one-sixth of the time required for the frequency sweep maneuver in Fig. 2. It might be possible to shorten the frequency sweep maneuver and maintain its effectiveness by omitting the lower-frequency portions of the maneuver because only the relatively high-frequency closed-loop short period dynamics were being identified. However, even in this case, the maneuver would probably need to be repeated to obtain good results from the CIFER method, whereas the EE/OE method gives accurate results based on measured data from a single, relatively short maneuver.

The CIFER method produces a good measure of the linearity of the input–output relationship as a function of frequency, called the coherence. A coherence value of one represents a perfectly linear relationship between the input and output. Figure 5 shows the coherence for the frequency sweep input, the single 2-1-1 maneuver, and the multiple concatenated 2-1-1 maneuvers. The coherence was degraded for most of the frequency range using a single 2-1-1

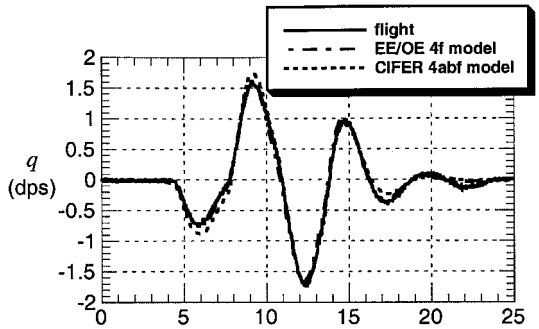

a)

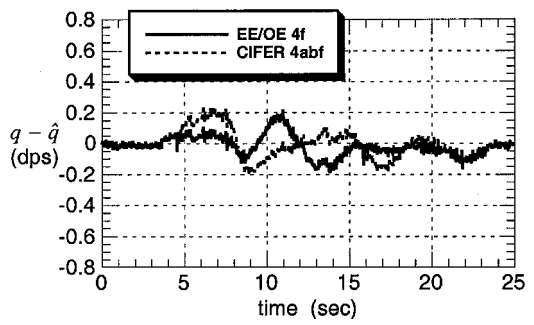

b)

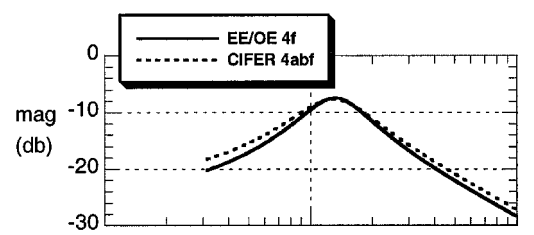

c)

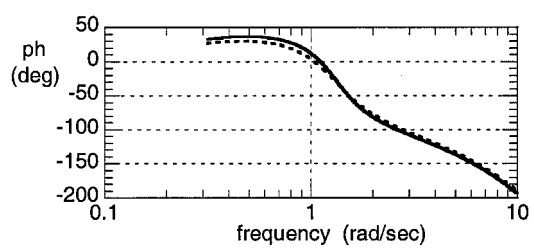

d)

Fig. 4 CIFER results for linked 2-1-1 maneuvers 22_4a, 22_4b, and 22_4f.

maneuver, but improved with the additional information contained in either the concatenated 2-1-1 maneuvers or the frequency sweep. Figures 5a–5c indicate that only the frequency sweep contains data for low-frequency mode identification. Figure 5 and the results shown earlier indicate that the quality of CIFER models was related to the coherence over the frequency band used for LOES modeling. The EE/OE method does not have this characteristic because no spectral estimation is done.

Because the EE/OE method does not use spectral estimates, the coherence is not used. Instead, the adequacy of the LOES model structure is assessed in the EE step, using methods and metrics typically employed for regression modeling problems, such as estimated parameter standard errors, the multiple correlation coefficient R^2, F ratios, prediction error metrics, and residual analysis.[16] The closest analog to the coherence is the multiple correlation coefficient R^2, which is the ratio of the squared variation of the model values about the mean to the squared variation of the measurements about the mean. The other methods and metrics are, in general, less direct and quantitative compared to the coherence.

Figure 6 shows a similar 2-1-1 maneuver executed at approximately the same flight condition. In Fig. 6b, the LOES models identified in the preceding example (cf. Table 3) were used with the input shown in Fig. 6a to predict the pitch rate response. For this prediction case, the fidelity of the EE/OE and CIFER models was similar to what was seen in Figs. 3 and 4. Note that this is not really a prediction case for the CIFER 4abf model because the prediction maneuver shown in Fig. 6 is maneuver 22_4a, which was part of the data used to identify the CIFER 4abf model. This is a prediction case for the EE/OE 4f and the CIFER 4f models. Figure 6 show excellent prediction capability for the EE/OE model identified from maneuver 22_4f alone.

Table 4 Tu-144LL LOES modeling summary results: phase 2 flight tests, longitudinal

Parameter	Supersonic cruise	Transonic cruise	Canard extended approach
Maneuver(s)	f23_1a	f20_4b,c,d	f20_4h,i,j
M_0	1.93	0.88	0.34
α_0, deg	4.8	5.8	8.1
h_0, 10^3 ft	53.4	29.7	7.0
w, lbf	3.35×10^5	3.22×10^5	3.04×10^5
I_y, slug · ft^2	1.44×10^7	1.37×10^7	1.28×10^7
$x_{\text{c.g.}}$	$0.46\bar{c}$	$0.46\bar{c}$	$0.41\bar{c}$
Landing gear	Retracted	Retracted	Extended
Canard	Retracted	Retracted	Extended
Nose, deg	0	0	17
b_1	0.353 ± 0.011	1.512 ± 0.080	0.626 ± 0.026
b_0	0.106 ± 0.006	1.894 ± 0.101	0.457 ± 0.154
a_1	0.932 ± 0.035	3.680 ± 0.182	1.741 ± 0.156
a_0	1.970 ± 0.035	7.246 ± 0.286	1.518 ± 0.380
τ_e	0.194 ± 0.014	0.280 ± 0.009	0.200 ± 0.008
$K_{\dot{\theta}}$	0.35	1.51	0.63
$1/T_{\theta_2}$	0.30	1.25	0.73
ζ_{SP}	0.33	0.68	0.71
ω_{SP}	1.40	2.69	1.23

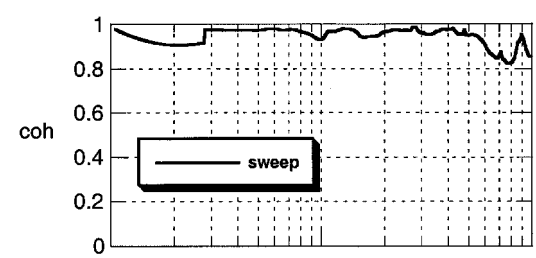

a)

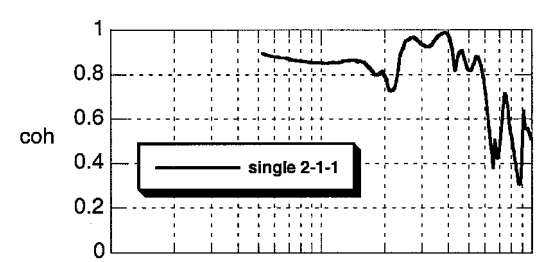

b)

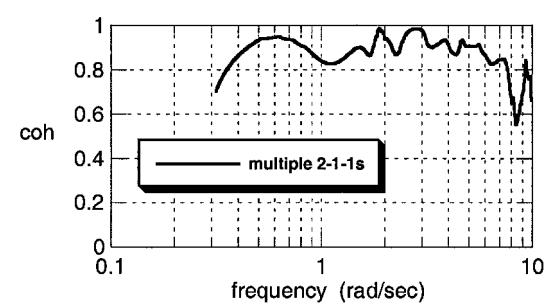

c)

Fig. 5 Coherence comparison.

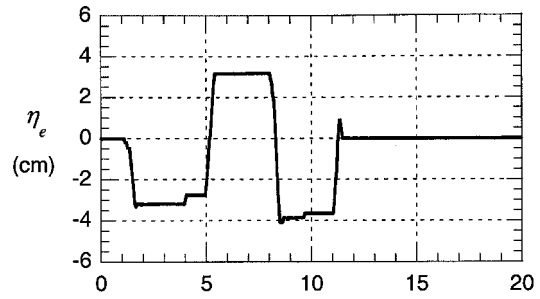

a)

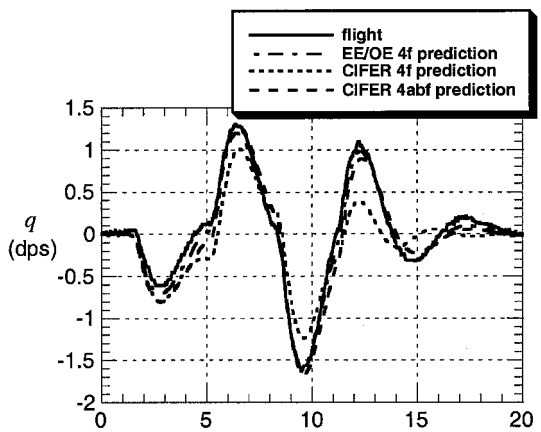

b)

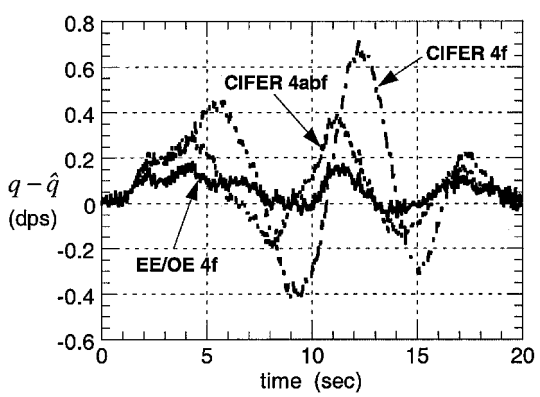

c)

Fig. 6 Multistep 2-1-1 prediction maneuver 22_4a, $\alpha_0 = 5.1$ deg, $M_0 = 1.91$, $x_{c.g.} = 0.46\bar{c}$, and $I_y = 1.44 \times 10^7$ slug · ft^2.

Figure 7 shows another longitudinal 2-1-1 maneuver, this time at transonic cruise, Mach 0.88. The model trace shown in Fig. 7b was generated using the LOES model of Eq. (4) with parameters estimated using the EE/OE method. Results for this case are given in the third column of Table 4. In Fig. 8, this identified LOES model was used for a prediction case at the same flight condition, with inverted polarity of the 2-1-1 longitudinal stick input. Figure 8 demonstrates the excellent prediction capability for LOES models identified using the EE/OE method. The prediction results for this case also indicate that the LOES model was not sensitive to input polarity, which supports the idea that the LOES model is an accurate representation of the Tu-144LL closed-loop short period dynamics at this flight condition.

The next case was multiple-input/multiple-output lateral/directional LOES modeling at supersonic cruise. Roll rate and yaw rate outputs were used with both lateral stick and rudder pedal inputs, in the model structure of Eqs. (5) and (6). Data from both a rudder pedal sweep and a lateral stick sweep maneuver were combined in the frequency domain for LOES modeling using the EE/OE method. Figure 9 shows input–output data from the lateral stick sweep maneuver. The model fit to the data in both the time domain and the frequency domain was excellent, demonstrating that the EE/OE method can be successfully used for multiple-input/multiple-output lateral/directional LOES modeling. The quality of the time domain fit to the rudder pedal sweep maneuver (not shown) was similar. The second column of Table 5 contains results for this case.

Longitudinal and lateral/directional LOES modeling results at several different flight conditions, based on measured data from the Tu-144LL phase 2 flights, are summarized in Tables 4 and 5. The flight conditions are as follows: canard-extended approach at Mach 0.34, transonic cruise at Mach 0.88, and supersonic cruise

Table 5 Tu-144LL LOES modeling summary results: phase 2 flight tests, lateral/directional

Parameter	Supersonic cruise
Maneuver(s)	f23_2a,3a
M_0	1.94
α_0, deg	4.6
h_0, 10^3 ft	53.9
w, lbf	3.13×10^5
I_x, slug · ft^2	1.17×10^6
I_z, slug · ft^2	1.51×10^7
I_{xz}, slug · ft^2	-9.75×10^4
$x_{c.g.}$	$0.46\bar{c}$
Landing gear	Retracted
Canard	Retracted
Nose, deg	0
c_2	4.785 ± 0.274
c_1	3.464 ± 0.116
c_0	6.981 ± 0.425
d_2	-1.406 ± 0.119
d_1	0.490 ± 0.184
d_0	2.377 ± 0.158
e_2	9.514 ± 0.521
e_1	1.052 ± 0.113
e_0	12.676 ± 0.717
f_2	0.278 ± 0.060
f_1	1.107 ± 0.068
f_0	0.263 ± 0.033
g_2	0.015 ± 0.041
g_1	-0.379 ± 0.042
g_0	1.082 ± 0.084
τ_a	0.221 ± 0.039
τ_r	0.218 ± 0.010
ζ_{DR}	0.169
ω_{DR}	1.27
$1/T_R$	4.34

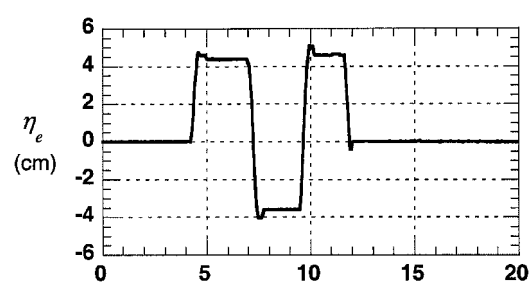

a)

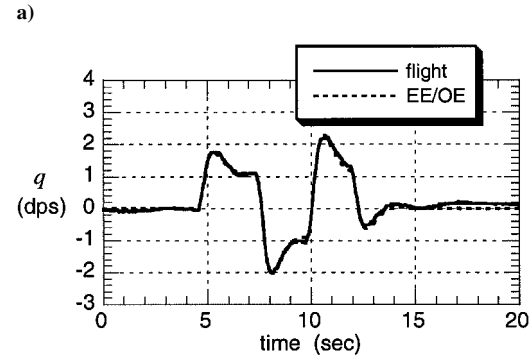

b)

Fig. 7 Multistep 2-1-1 identification maneuver 20_4d, $\alpha_0 = 5.8$ deg, $M_0 = 0.88$, $x_{c.g.} = 0.46\bar{c}$, and $I_y = 1.37 \times 10^7$ slug · ft^2.

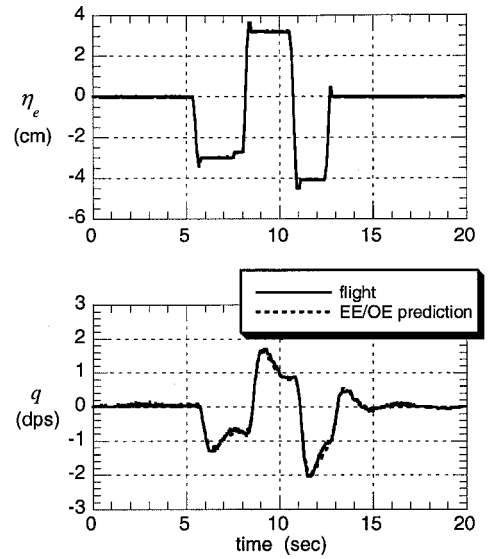

Fig. 8 Multistep 2-1-1 prediction maneuver 20_4f, $\alpha_0 = 5.8$ deg, $M_0 = 0.88$, $x_{c.g.} = 0.46\bar{c}$, and $I_y = 1.37 \times 10^7$ slug · ft^2.

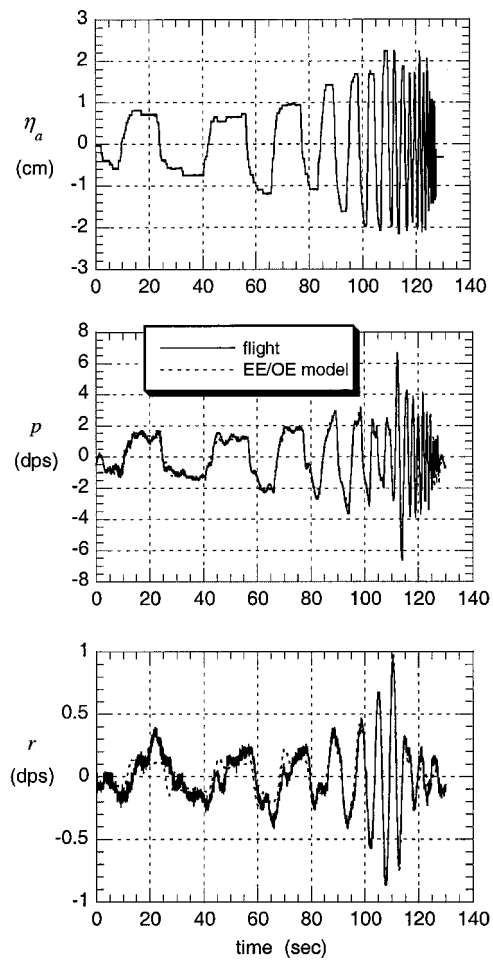

Fig. 9 Frequency sweep maneuver 23_2a, $\alpha_0 = 4.6$ deg, $M_0 = 1.94$, $x_{c.g.} = 0.46\bar{c}$, $I_x = 1.17 \times 10^6$ slug · ft^2, $I_z = 1.51 \times 10^7$ slug · ft^2, and $I_{xz} = -9.75 \times 10^4$ slug · ft^2.

at Mach 1.93. All LOES modeling results in Tables 4 and 5 were obtained using the EE/OE method. More than one maneuver was used in cases where the flight conditions for the maneuvers were nearly the same. This is indicated by the maneuver(s) listed for each flight condition.

Based on the LOES parameter estimates, excluding the specifications on the equivalent time delay, the Military Standard in Ref. 4 indicated that the aircraft closed-loop dynamics exhibited level 2 longitudinal flying qualities for supersonic cruise, transonic cruise, and canard-extended approach, and level 1 lateral/directional flying qualities for supersonic cruise. These flying qualities levels were consistent with qualitative comments from the evaluation pilots.[8]

LOES modeling was also done using the EE/OE method for several longitudinal cases with a 150-ms delay removed from the pitch rate measurement. This was the estimated time delay that could be reasonably attributed to instrumentation time skew based on control surface deflection and pitch rate measurements for the multistep maneuvers, allowing for normal pitch rate response delay on a large aircraft. For pitch rate data with a 150-ms time delay removed, estimated LOES model parameters were essentially unchanged, except that the equivalent time delay estimate was roughly 150 ms smaller. If estimated equivalent time delays were reduced by 150 ms for all longitudinal and lateral/directional cases in Table 5, the Military Standard in Ref. 4 indicated that the aircraft closed-loop dynamics exhibited level 2 longitudinal flying qualities and level 1 lateral/directional flying qualities, again in concurrence with qualitative pilot opinion.[8]

Conclusions

This work was concerned with accurately identifying closed-loop LOES models from flight-test data for the Tu-144LL supersonic transport aircraft. LOES models are linear models with input time delay, used to characterize closed-loop aircraft response to pilot inputs. Data analysis was done in the frequency domain using two methods: a two-step EE/OE technique using a high-accuracy Fourier transform with selectable frequency range and resolution, and a least-squares fit to Bode plot data generated from spectral estimates (CIFER). Details of the methods were discussed and compared. Both methods identified accurate LOES models using data from a frequency sweep maneuver or multiple concatenated multistep maneuvers. For single multistep maneuvers, only the EE/OE method produced accurate LOES model fits with good prediction capability.

The EE/OE modeling technique was applied to phase 2 flight-test data from the Tu-144LL aircraft to identify closed-loop LOES models for various flight conditions and configurations, including transonic cruise, canard-extended approach, and supersonic cruise. Longitudinal and lateral/directional LOES modeling results were computed and tabulated. The lateral/directional results demonstrated the capability to identify accurate multiple-input/multiple-output LOES models from flight-test data. Although anomalies in the measured data limited the output measurements to only angular rate data, identified LOES models showed excellent fits to the data in the time domain and frequency domain and exhibited excellent prediction capability. All LOES modeling in this work was done using only measurements for pilot inputs and body-axis angular rate outputs, demonstrating that this type of analysis can be done successfully with minimal instrumentation.

The results shown suggest that the EE/OE method can be used in conjunction with relatively short multistep inputs to decrease flight-test time required to collect data for LOES model identification, compared to using frequency sweeps. There are cases where frequency sweeps are difficult to implement, such as flight at high angles of attack, drop model flight tests, and flexible aircraft with significant structural responses in the frequency band of the sweep. For such cases, the EE/OE method could expand the range of applicability and usefulness of the LOES concept by allowing the use of short multistep inputs. The applicability might also extend to data from normal flight operations, such as landing or tracking tasks.

Acknowledgments

Flight-test maneuvers were flown by Sergei Borisov from Tupolev Aircraft Company, Robert Rivers from NASA Langley Research Center, and Gordon Fullerton from NASA Dryden Flight Research Center. Flight tests were carried out at the Tupolev Aircraft Company flight research facility by personnel from Tupolev ANTK, The Boeing Company, NASA Dryden Flight Research Center, and NASA Langley Research Center. Technical consulting on the CIFER results was provided by Mark Tischler from NASA Ames Research Center.

References

[1]Curry, T. J., "Estimation of Handling Qualities Parameters of the Tu-144 Supersonic Transport Aircraft from Flight Test Data," NASA CR-2000-210290, Aug. 2000.

[2]Morelli, E. A., "Identification of Low Order Equivalent System Models from Flight Test Data," NASA TM-2000-210117, Aug. 2000.

[3]Klein, V., "Aircraft Parameter Estimation in Frequency Domain," AIAA Paper 78-1344, Aug. 1978.

[4]"Military Standard—Flying Qualities of Piloted Aircraft," MIL-STD-1797A, Jan. 1990.

[5]Hodgkinson, J., LaManna, W. J., and Heyde, J. L., "Handling Qualities of Aircraft with Stability and Control Augmentation Systems—A Fundamental Approach," *Aeronautical Journal*, Vol. 80, No. 782, Feb. 1976, pp. 75–81.

[6]Mitchell, D. G., and Hoh, R. H., "Low-Order Approaches to High-Order Systems: Problems and Promises," *Journal of Guidance, Control, and Dynamics*, Vol. 5, No. 5, 1982, pp. 482–489.

[7]Hodgkinson, J., Snyder, R. C., and Smith, R. E., "Equivalent System Verification and Evaluation of Augmentation Effects on Fighter Approach and Landing Flying Qualities," AFWAL-TR-81-3116, Sept. 1981.

[8]Rivers, R. A., Jackson, E. B., Fullerton, C. G., Cox, T. H., and Princen, N. H., "A Qualitative Piloted Evaluation of the Tupolev Tu-144 Supersonic Transport," NASA TM-2000-209850, Feb. 2000.

[9]Morelli, E. A., "High Accuracy Evaluation of the Finite Fourier Transform Using Sampled Data," NASA TM 110340, June 1997.

[10]Tischler, M. B., and Cauffman, M. G., "Frequency-Response Method for Rotorcraft System Identification: Flight Applications to BO-105 Coupled Rotor/Fuselage Dynamics," *Journal of the American Helicopter Society*, Vol. 37, No. 3, 1992, pp. 3–17.

[11]Tischler, M. B., and Cauffman, M. G., *Comprehensive Identification from Frequency Responses, Vol. 1—Class Notes*, NASA CP 10149, 1994.

[12]Tischler, M. B., and Cauffman, M. G., *Comprehensive Identification from Frequency Responses, Vol. 2—User's Manual*, NASA CP 10150, 1994.

[13]Maine, R. E., and Iliff, K. W., "Application of Parameter Estimation to Aircraft Stability and Control—The Output-Error Approach," NASA RP 1168, June 1986.

[14]Morelli, E. A., and Klein, V., "Determining the Accuracy of Maximum Likelihood Parameter Estimates with Colored Residuals," NASA CR 194893, March 1994.

[15]Klein, V., and Morgan, D. R., "Estimation of Bias Errors in Measured Airplane Responses Using Maximum Likelihood Method," NASA TM 89059, Jan. 1987.

[16]Morelli, E. A., "System Identification Programs for AirCraft (SIDPAC)," AIAA Paper 2002-4704, Aug. 2002.

[17]Taylor, L. W., Jr., and Iliff, K. W., "Systems Identification Using a Modified Newton–Raphson Method—A FORTRAN Program," NASA TN D-6734, May 1972.